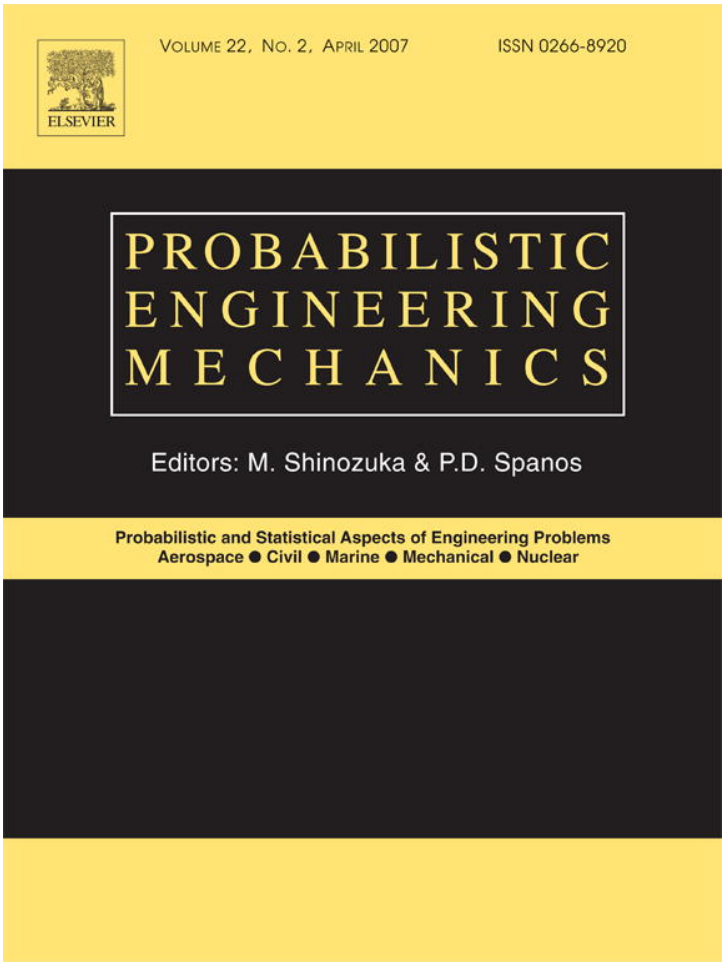

Available online at www.sciencedirect.com
ScienceDirect
Probabilistic Engineering Mechanics 22 (2007) 194–205
PROBABILISTIC ENGINEERING MECHANICS
www.elsevier.com/locate/probengmech

Collocation-based stochastic finite element analysis for random field problems

Shuping Huang, Sankaran Mahadevan*, Ramesh Rebba

Vanderbilt University, Nashville, TN 37235, United States

Received 12 December 2003; received in revised form 30 October 2006; accepted 8 November 2006
Available online 18 December 2006

Abstract

A stochastic response surface method (SRSM) which has been previously proposed for problems dealing only with random variables is extended in this paper for problems in which physical properties exhibit spatial random variation and may be modeled as random fields. The formalism of the extended SRSM is similar to the spectral stochastic finite element method (SSFEM) in the sense that both of them utilize Karhunen–Loeve (K–L) expansion to represent the input, and polynomial chaos expansion to represent the output. However, the coefficients in the polynomial chaos expansion are calculated using a probabilistic collocation approach in SRSM. This strategy helps us to decouple the finite element and stochastic computations, and the finite element code can be treated as a black box, as in the case of a commercial code. The collocation-based SRSM approach is compared in this paper with an existing analytical SSFEM approach, which uses a Galerkin-based weighted residual formulation, and with a black-box SSFEM approach, which uses Latin Hypercube sampling for the design of experiments. Numerical examples are used to illustrate the features of the extended SRSM and to compare its efficiency and accuracy with the existing analytical and black-box versions of SSFEM.

Keywords: Stochastic finite elements; Response surface; Karhunen–Loeve expansion; Polynomial chaos; Galerkin; Collocation

1. Introduction

Many structural parameters such as material properties, geometric parameters and loads show random variability in spatial distribution as well as in intensity, and may be modeled as random fields rather than random variables. Mathematically, this kind of problem is characterized by stochastic partial differential equations for which the input data are stochastic. Due to the complexity of the engineering system, closed-form solutions of even the simplest governing equations are not possible when defined over mildly irregular domains. Therefore, the treatment of randomness in the physical system needs to be adapted to the implementation of the finite element method which can deal with geometrical complexity. In many instances, suitable modifications have been added to the finite element method to account for the stochastic effects. These techniques are called stochastic finite element methods which are used to solve stochastic partial differential equations.

Various stochastic finite element methods have been proposed in the literature. Perturbation [20,11] and Neumann expansion [18] work well when the variability is not large. Monte Carlo simulation methods are accurate and widely applicable but time-consuming. When the models are large, or when there are many parameters, even the best of Monte Carlo or importance sampling methods can be prohibitively expensive. The application of response surface methods to problems involving random fields is also not easy due to the large number of random variables into which a continuous random field is reduced by discretization. The spectral stochastic finite element method (SSFEM) developed by Ghanem and Spanos [1] appears to be a suitable technique for the solution of complex, general problems in probabilistic mechanics. It is capable of handling much higher fluctuations. However, this method requires access to the governing model equations. Furthermore, the resulting system of equations to be solved for the unknown response is much larger than those

* Corresponding author. Tel.: +1 615 322 3040; fax: +1 615 322 3365.
E-mail address: sankaran.mahadevan@vanderbilt.edu (S. Mahadevan).

0266-8920/$ - see front matter © 2006 Elsevier Ltd. All rights reserved.
doi:10.1016/j.probengmech.2006.11.004

from deterministic finite element analysis. For complicated large system problems, the system of equations in the spectral stochastic finite element method could be tremendously large. For example, if the deterministic system is of size $n \times n$, and the number of terms in the polynomial chaos expansion is N, then the size of the stochastic system would be $N \times n \times N \times n$. Although a new implementation of SSFEM [5], which is theoretically equivalent to the original SSFEM, has been developed for the purpose of utilizing commonly available FEM codes as a black box, this novel implementation of SSFEM (mentioned in this paper as black-box SSFEM) uses random sampling of the input and consequently a large number of FEM runs to get a stable estimate of the coefficients in the expansion of the solution. The original SSFEM [1] is referred to in this paper as analytical SSFEM, for the sake of comparison.

This paper presents a modified spectral stochastic finite element method. This methodology is based on the stochastic response surface method (SRSM) which has been previously proposed by Isukapalli et al. [8] for problems dealing only with random variables. This paper extends SRSM to problems involving random fields or random processes. This methodology uses Karhunen–Loeve (K–L) expansion [19] and polynomial chaos ([1,23,22]) to construct a response surface as an efficient uncertainty propagation model. First, the input random field is discretized into standard random variables using the K–L expansion. The output is represented by a polynomial chaos expansion in terms of these standard random variables. The unknown coefficients of the polynomial chaos-based response surface are estimated based on the finite element model outputs at a set of collocation points in the sample space.

Compared to the conventional response surface, the stochastic response surface has several advantages to justify using it as a more reliable metamodel. First, the polynomial chaos is a mean square convergent series expansion. It is optimal in the Fourier sense since it minimizes the mean square error from truncation after a finite number of terms in the series [1]. (A practical outcome of this is that the coefficients of the lower order terms stay stable as higher order terms are added to the response surface. The polynomial chaos-based response surface has this property, whereas conventional response surfaces do not.) Secondly, polynomial chaos in terms of the standard normal variables provides a complete orthogonal basis for the L^2 space (space for second order random function). Therefore any random function in the space can be represented by the polynomial chaos basis with corresponding coefficients. Thirdly, polynomial chaos is a Hermite polynomial of random variables. The roots of the Hermite polynomial provide efficient collocation points to evaluate the model output and compute the coefficients in the response surface.

The extended SRSM developed here for problems with random fields establishes an effective and general means for characterizing system response. The main elements are K–L expansion for efficient representation of the input random fields, and polynomial chaos for representation of the response. The former permits the optimal representation of the uncertainty in the input. The latter permits the representation of the response as a non-Gaussian random field so that any characteristic of the response desired by the analyst or designer can be directly established.

The formalism of the extended SRSM is similar to the spectral stochastic finite element method in the sense that both of them utilize Karhunen–Loeve expansion and polynomial chaos expansion to represent the input and output random fields respectively. However, the calculation of the coefficients in the polynomial chaos expansion is different in the two methods. Analytical SSFEM uses a probabilistic Galerkin approach while the proposed method uses a probabilistic collocation approach. Similar to the Galerkin and collocation methods which are weighted residual methods in deterministic numerical analysis, the probabilistic Galerkin and collocation methods are both weighted residual methods in the random domain. The approach can be viewed as an extension of deterministic computational analysis to the stochastic case, with an appropriate extension of the concept of weighted residual error minimization.

The sample points in the proposed method are chosen from collocation points which are roots of the Hermite polynomial basis. Among combinations of different roots, the collocation points are chosen from high probability regions. This selection procedure results in fewer function evaluations for high accuracy. Compared to the analytical version of SSFEM, the advantage of the extended SRSM is that the finite element code can be treated as a black box, as in the case of a commercial code. The proposed SRSM is also compared to a black-box version of SSFEM, and found to require less FEM evaluations for the same accuracy.

2. Spectral stochastic finite element method

The spectral stochastic finite element method (SSFEM) has been developed and applied to various problems. Detailed descriptions of SSFEM can be found in several papers [1,3,2,10,4,13,5]. The essential concepts of SSFEM are provided here, as it is necessary for understanding the modified method. The proposed stochastic response surface method for random field problems will be presented later in the next section.

2.1. Problem description

A standard form of a stochastic partial differential equation (SPDE) may be written as

$$K(u, \varpi(x, \theta))u = F(\theta) \tag{1}$$

where u denotes the solution of the problem, $\varpi(x, \theta)$ denotes the random material property and θ refers to the random events. The presence of stochasticity in either the system coefficient $\varpi(x, \theta)$ or source term $F(\theta)$ will render the solution u to be stochastic. There are two types of problems of interest here: one with a stochastic source term and deterministic system coefficients; the other with stochastic system coefficients and a deterministic source term. The proposed method can consider stochasticity in both system coefficients and source terms.

The main elements in SSFEM are K–L expansion-based representation of the input random fields, polynomial chaos

representation of the output, and calculation of the unknown coefficients by a Galerkin scheme in the random dimension. These concepts are summarized below.

2.2. Karhunen–Loeve expansion

A second order random process $\varpi(x,\theta)$ defined on a probability space (Ω, A, P) and indexed on a bounded domain D can be expanded as [19]

$$\varpi(x,\theta) = \overline{\varpi}(x) + \sum_{i=1}^{\infty} \sqrt{\lambda_i}\xi_i(\theta) f_i(x) \tag{2}$$

in which λ_i and $f_i(x)$ are the Eigenvalues and Eigenfunctions of the covariance function $C(x_1, x_2)$. By definition, $C(x_1, x_2)$ is bounded, symmetric and positive definite. Following Mercer's Theorem [19], it has the following spectral or Eigen-decomposition:

$$C(x_1, x_2) = \sum_{i=1}^{\infty} \lambda_i f_i(x_1) f_i(x_2) \tag{3}$$

which has a countable number of Eigenvalues and the associated Eigenfunctions obtained from the solutions of the integral equation

$$\int_D C(x_1, x_2) f_i(x_2) \mathrm{d}x_2 = \lambda_i f_i(x_1). \tag{4}$$

Eq. (4) arises from the fact that the Eigenfunctions form a complete orthogonal set satisfying the equation:

$$\int_D f_i(x) f_j(x) \mathrm{d}x = \delta_{ij} \tag{5}$$

where δ_{ij} is the Kronecker-delta function.

The parameter $\xi_i(\theta)$ in Eq. (5) is a set of uncorrelated random variables which can be expressed as:

$$\xi_i(\theta) = \frac{1}{\sqrt{\lambda_i}} \int_D [\varpi(x,\theta) - \overline{\varpi}(x)] f_i(x) \mathrm{d}x \tag{6}$$

with mean and covariance function given by:

$$E[\xi_i(\theta)] = 0 \tag{7a}$$

$$E[\xi_i(\theta)\xi_j(\theta)] = \delta_{ij}. \tag{7b}$$

The K–L expansion in Eq. (2) provides a second-moment characterization in terms of uncorrelated random variables and deterministic orthogonal functions. It is known to converge in the mean square sense for any distribution of $\varpi(x,\theta)$ [19]. For practical implementation, the series is approximated by a finite number of terms, say M, giving:

$$\varpi_M(x,\theta) = \overline{\varpi}(x) + \sum_{i=1}^{M} \sqrt{\lambda_i}\xi_i(\theta) f_i(x). \tag{8}$$

In physical systems it can be expected that material properties vary smoothly at the scale of interest for most of the applications. Therefore, just a few terms of K–L expansion can capture most of the uncertainty in the process.

If $\varpi(x,\theta)$ is further restricted to a zero-mean Gaussian process, then the appropriate choice of $\{\xi_1(\theta), \xi_2(\theta)\ldots\}$ is a vector of zero-mean uncorrelated Gaussian random variables.

2.3. Polynomial chaos expansion

Since the output is a function of the input fields, it can be expressed by a nonlinear function of the set of random variables which are used to represent input stochasticity. The function of Gaussian variables which is known as polynomial chaos is given by

$$\begin{aligned} u(\theta) = a_o \Gamma_0 &+ \sum_{i_1=1}^{n} a_{i_1} \Gamma_1(\xi_{i_1}(\theta)) \\ &+ \sum_{i_1=1}^{n} \sum_{i_2=1}^{i_1} a_{i_1 i_2} \Gamma_2(\xi_{i_1}(\theta), \xi_{i_2}(\theta)) \\ &+ \sum_{i_1=1}^{n} \sum_{i_2=1}^{i_1} \sum_{i_3=1}^{i_2} a_{i_1 i_2 i_3} \Gamma_3(\xi_{i_1}(\theta), \xi_{i_2}(\theta), \xi_{i_3}(\theta)) + \cdots \end{aligned} \tag{9}$$

where $\Gamma_p(\xi_{i_1}, \ldots, \xi_{i_p})$ denotes the polynomial chaos of order p in terms of the multi-dimensional random variables $\{\xi_{i_k}\}_{k=1}^{M}$. The polynomial chaos is defined in terms of Hermite polynomials as

$$\Gamma_p(\xi_{i_1}, \ldots, \xi_{i_M}) = (-1)^p \mathrm{e}^{\frac{1}{2}\xi^T\xi} \frac{\partial^M}{\partial\xi_{i_1}\ldots\partial\xi_{i_M}} \mathrm{e}^{-\frac{1}{2}\xi^T\xi}. \tag{10}$$

This is the same as an M-dimensional Gaussian joint probability density function.

For notational simplicity, Eq. (9) is rewritten as

$$u(\theta) = \sum_{j=0}^{N} u_j \Phi_j(\xi(\theta)) \tag{11}$$

where there is a correspondence between $\Gamma_p(\xi_{i_1}, \ldots, \xi_{i_n})$ and $\Phi(\xi)$ and their corresponding coefficients. The orthogonality of the polynomial chaos is of the form:

$$\langle \Phi_i \Phi_j \rangle = \langle \Phi_i^2 \rangle \delta_{ij} \tag{12}$$

where δ_{ij} is the Kronecker-delta function. The polynomial chaoses of order greater than one have zero mean; polynomials of different order are orthogonal to each other, and so are polynomials of the same order but with different arguments. Details for calculating polynomial chaos can be found in Ref. [1]. The series could be truncated to a finite number of terms. The accuracy of the computational model increases as the order of the polynomial chaos expansion increases. For example, the second and third order Hermite polynomials are as follows:

$$\{\Phi\} = \{1, \xi_1, \xi_2, \xi_1^2 - 1, \xi_1\xi_2, \xi_1^2 - 1\} \tag{13}$$

$$\begin{aligned} \{\Phi\} = \{&1, \xi_1, \xi_2, \xi_1^2 - 1, \xi_1\xi_2, \xi_1^2 - 1, \xi_1^3 - 3\xi_1, \\ &\xi_1^2\xi_2 - \xi_2, \xi_2^2\xi_1 - \xi_1, \xi_2^3 - 3\xi_2\}. \end{aligned} \tag{14}$$

2.4. Analytical spectral stochastic finite element formulation

Substituting Eqs. (8) and (11) into the equation of equilibrium (Eq. (1)) yields

$$\sum_{j=0}^{N} \Phi_j K(u, \xi(\theta)) u_j = F(\theta). \tag{15}$$

The error in the above equation can be minimized using the Galerkin method which requires the error to be orthogonal to the basis functions in the approximation space:

$$\sum_{j=0}^{N} \langle \Phi_k \Phi_j K(u, \xi(\theta)) \rangle u_j = \langle \Phi_k F(\theta) \rangle, \quad k = 0, 1, \ldots N. \tag{16}$$

The random coefficients matrix K can be expanded into a polynomial of the form

$$K = \sum_{0}^{M} \xi_i K_i, \quad K_i = \frac{\langle \xi_i K \rangle}{\langle \xi_i^2 \rangle}. \tag{17}$$

Eq. (16) becomes

$$\sum_{i=0}^{M} \sum_{j=0}^{N} \langle \xi_i \Phi_j \Phi_k \rangle K_i u_j = \langle \Phi_k F \rangle, \quad k = 0, 1, \ldots N. \tag{18}$$

The coefficients of the response on the left hand side of Eq. (18) can be assembled into a matrix of size $(N+1) \times n$ by $(N+1) \times n$ of the form

$$\begin{bmatrix} K^{(00)} & K^{(01)} & \cdots & K^{(0N)} \\ K^{(10)} & K^{(11)} & & \\ & \ddots & & \\ \vdots & & K^{(jk)} & \\ K^{(N0)} & & & K^{(NN)} \end{bmatrix} \tag{19}$$

where

$$K^{(jk)} = \sum_{i=1}^{M} \langle \xi_i \Phi_j \Phi_k \rangle K_i. \tag{20}$$

This is an $n \times n$ matrix in which n is the number of degrees of freedom in the physical domain. The index i denotes the ith term in the K–L expansion and K_i is the global stiffness matrix associated with the ith term ($i = 1$ to M). The element stiffness matrix is obtained as

$$k_i^{(lm)} = \int_e \sqrt{\lambda} f_i(x) \frac{\mathrm{d}^2}{\mathrm{d}x^2}(P_l(x)) \frac{\mathrm{d}^2}{\mathrm{d}x^2}(P_m(x)) \mathrm{d}x. \tag{21}$$

Eq. (18) can be rewritten as

$$\sum_{j=0}^{N} K_{jk} u_j = F_k. \tag{22}$$

Eq. (22) is a set of $N + 1$ equations, each of which is of the same size as in the deterministic problem. The size of the global stiffness matrix K is $(N + 1) \times n$ by $(N + 1) \times n$ if the number of degrees of freedom in the physical domain is n.

Table 1
Number of terms in the M-dimensional pth order polynomial chaos expansion

	$M = 1$	$M = 2$	$M = 3$	$M = 4$
$p = 1$	2	3	4	5
$p = 2$	3	6	10	15
$p = 3$	4	10	20	35
$p = 4$	5	15	35	70

Once the coefficients u_j of Eq. (11) are obtained by solving Eq. (22), the statistics of the response such as mean and standard deviation can be estimated as

$$\langle u \rangle = u_0; \quad \mathrm{Cov}(u, u) = \sum_{j=0}^{P} \langle \Phi_j \Phi_j \rangle u_j u_j^H. \tag{23}$$

From the above discussion, it is seen that in SSFEM, the representation of the random fields in the context of the finite element procedure has the effect of adding extra dimensions to a problem with n degrees of freedom. The polynomial chaos, which is used to discretize the random dimension, contributes a factor of $(N + 1)$ to the size of the problem. Coupling this new discretization with the finite element spatial discretization in a discrete system, the problem size becomes $(N + 1) \times n \times (N + 1) \times n$. This increases the computational cost during the creation and solution of the system coefficient matrix. This is further affected by the number of terms (M) used in the K–L expansion of the input random fields due to the following relation:

$$N = \sum_{s=1}^{p} \frac{1}{s!} \prod_{r=0}^{s-1} (M + r). \tag{24}$$

Table 1 gives some explicit values of N for given dimension of the polynomial chaos M and the order of the polynomial chaos p. The price is justified, since the SFEM formulation attempts to answer a more comprehensive question than deterministic FEM. While deterministic FEM predicts the behavior of a particular realization of the problem, SFEM seeks a complete probabilistic characterization of the solution.

However, it is seen from Eq. (21) that formulating the element stiffness requires access to the governing model equations. Furthermore, the resulting system of equations to be solved for the unknown response is much larger than those from deterministic finite element analysis. The size of the problem controls the computational efficiency. For complicated large system problems, the system of equations in the spectral stochastic finite element method could be tremendously large.

2.5. Black-box spectral stochastic finite element formulation

The coefficients in Eq. (11) can also be evaluated by another method [5], referred to in this paper as the black-box SSFEM. Given the orthogonality of the polynomial chaos basis $\Phi(\xi)$, the coefficients in the expansion in Eq. (11) can be computed as generalized Fourier coefficients according to the following

expression

$$u_j = \frac{\langle \Phi_j u \rangle}{\langle \Phi_j^2 \rangle}. \tag{25}$$

For each realization of the set of basic random variables ξ_i, the realization of the input representing the material property is obtained by Eq. (2). Then the realization of the output (solution) is obtained by solving the finite element system (one FEM run). The realization of the solution is multiplied by each of the realizations of $\Phi(\xi)$ and Eq. (25) is evaluated, thus leading to an estimate of the coefficients in the expansion in Eq. (11). Basic Monte Carlo sampling and other variance reduction sampling techniques such as Latin Hypercube sampling [12,7] may be used for generating the input realizations.

The black-box SSFEM is developed for the purpose of utilizing commonly available FEM codes. However, it uses random sampling of the input and consequently a large number of FEM runs to get a stable estimate of the coefficients in the expansion of the solution. Therefore, a modified spectral stochastic finite element method is proposed in the next section, based on a probabilistic collocation approach. The proposed method preserves the benefits of expansions in SSFEM but uses a different error minimization process for the calculation of the unknown coefficients in the polynomial chaos. Also, the deterministic finite element analysis can be treated as a black box, as in the case of commercial codes. This formulation overcomes the shortcomings of analytical SSFEM with respect to programming and computational effort. When compared to the black-box SSFEM, the proposed collocation-based method usually requires much fewer samples to calculate the coefficients in the solution expansion. The reason is that they are based on different sampling mechanisms. In black-box SSFEM, sample points are selected according to some variation of random sampling rule i.e. basic Monte Carlo, Latin Hypercube sampling etc. while in SRSM, the sample points are selected at collocation points which correspond to regions of high probability. Details are given in the next section.

3. Collocation-based SSFEM: stochastic response surface method (SRSM)

The output from the analytical SSFEM can be viewed as a stochastic response surface in which the coefficients are calculated by the Galerkin method. Similar to the Galerkin method, the collocation method is another weighted residual minimization process in numerical analysis. It has been mathematically proved that an "optimal" collocation method with accuracy comparable to or even equal to the accuracy of the Galerkin method is obtained when the collocation points are selected at the zeros of the orthogonal polynomials used in the approximation [21]. If we extend the deterministic numerical analysis to the stochastic case, the relationship between the proposed method and SSFEM is analogous to the relationship between the collocation and the Galerkin methods in deterministic numerical analysis. In the stochastic case, the response, which is a random function, is approximated by a polynomial chaos-based response surface in both methods. The polynomial chaos is nothing but Hermite polynomials in terms of random functions (random variables). The probabilistic collocation points are therefore selected as roots of Hermite polynomials. Details of probabilistic collocation are given by Tatang et al. [17]. The collocation method is easier to implement but in general a little less accurate, whereas the Galerkin method is more accurate but cumbersome to implement [21]. In analytical SSFEM, in which the probabilistic Galerkin approach is pursued, the probabilistic analysis and FEM analysis are done together. Therefore, accessing the FEM code is necessary. Whereas in SRSM, in which probabilistic collocation is pursued, the FEM code can be treated as a black box.

The other two elements in SSFEM, K–L expansion representation of the input random fields and polynomial chaos projection of the response, remain the same.

3.1. Steps of SRSM

This method was first proposed by Isukapalli et al. [8]. However, the method was only limited to problems with random variables. In this paper, SRSM is extended to problems with random fields by using the K–L expansion. A general procedure of SRSM for random field problems is briefly summarized below:

(a) Representation of random process inputs in terms of Standard Random Variables (SRVs) by K–L expansion.
(b) Expression of model outputs in chaos series expansion. Once the inputs are expressed as functions of the selected SRVs, the output quantities can also be represented as functions of the same set of SRVs. If the SRVs are Gaussian, the chaos for the output is a Hermite polynomial of Gaussian variables, which is polynomial chaos. If the SRVs are non-Gaussian, the output can be expressed by Askey-chaos in terms of non-Gaussian variables. In this paper, only Gaussian fields are considered.
(c) Estimation of the unknown coefficients in the series expansion. The improved probabilistic collocation method [8] is used to minimize the residual in the random dimension by requiring the residual at the collocation points equal to zero. The model outputs are computed at a set of collocation points and used to estimate the coefficients. These collocation points are the roots of the Hermite polynomial of a higher order. This way of selecting collocation points would capture points from regions of high probability [17].
(d) Calculation of the statistics of the output which has been cast as a response surface in terms of a chaos expansion. The statistics of the response can be estimated with the response surface using either Monte Carlo simulation or analytical approximation.

Note that in the case of Gaussian random fields, the only difference between SSFEM and SRSM is in step (c) above, i.e., the calculation of the unknown coefficients in the polynomial chaos-based response surface.

3.2. Probabilistic collocation

The unknown coefficients in the polynomial chaos expansion can be obtained by a probabilistic collocation method. This method imposes the requirement that the estimates of model outputs be exact at a set of collocation points in the sample space, thus making the residual at those points equal to zero. The unknown coefficients are estimated by equating model outputs and the corresponding polynomial chaos expansions at a set of collocation points in the parameter space. The number of collocation points should be at least equal to the number of unknown coefficients to be found. Thus, for each response quantity, a set of linear equations results with the coefficients as the unknowns; these equations can be readily solved using linear solvers. The collocation points are the roots of a Hermite polynomial of one order higher than the order of polynomial expansion. This idea of selection is identical to Gaussian quadrature for estimating integrals. In Gaussian quadrature, the integral is approximated as a summation with no error by using the roots of the next higher order polynomial. Similarly, the collocation points are selected as the roots of the next higher order polynomial. Because the polynomial chaos is the Hermite polynomial of the Gaussian variables, the collocation points are roots of the Hermite polynomial. For example, the first to fifth order Hermite polynomials are

$$H_1(\xi) = \xi \tag{26a}$$

$$H_2(\xi) = \xi^2 - 1 \tag{26b}$$

$$H_3(\xi) = \xi^3 - 3\xi \tag{26c}$$

$$H_4(\xi) = \xi^4 - 6\xi^2 + 3 \tag{26d}$$

$$H_5(\xi) = \xi^5 - 10\xi^3 + 15\xi. \tag{26e}$$

The collocation points for the second order response surface are combinations of the roots of the third order Hermite polynomial $(-\sqrt{3}, 0, +\sqrt{3})$ and the collocation points for the third order response surface are combinations of the roots of the fourth order Hermite polynomial (± 0.7404, ± 2.3333) as shown in Table 2.

However, the collocation method is usually unstable, and the approximation result is dependent on the selection of the collocation points. In this study, a regression-based modified collocation approach is used to improve the accuracy. The number of collocation points used by the regression is more than the number of the unknown coefficients, thus reducing the effect of each individual point. For example, a second order response surface is constructed in this paper with 9 sample collocation points and a third order response surface with 17 sample collocation points, even though only 6 and 10 coefficients are needed respectively.

The collocation points are selected from combinations of the roots of a Hermite polynomial of one order higher than the order of the response surface. The selection is also expected to capture regions of high probability [17]. Fig. 1 illustrates this idea. The larger deviation of response of the approximate model from the response of the actual model occurs in the lower probability region and therefore produces only a small error.

Table 2
Collocation points as samples for the regression analysis

Pt	Second order		Third order	
	ξ_1	ξ_2	ξ_1	ξ_2
1	0	0	0	0
2	1.732	0	2.3333	0
3	0	1.732	0	2.3333
4	−1.732	0	−2.3333	0
5	0	−1.732	0	−2.3333
6	1.732	−1.732	0.7417	0
7	−1.732	1.732	0	0.7417
8	1.732	1.732	−0.7417	0
9	−1.732	−1.732	0	−0.7417
10			0.7417	0.7417
11			−0.7417	−0.7417
12			−0.7417	0.7417
13			0.7417	−0.7417
14			2.3333	0.7417
15			0.7417	2.3333
16			2.3333	−0.7417
17			−0.7417	2.3333

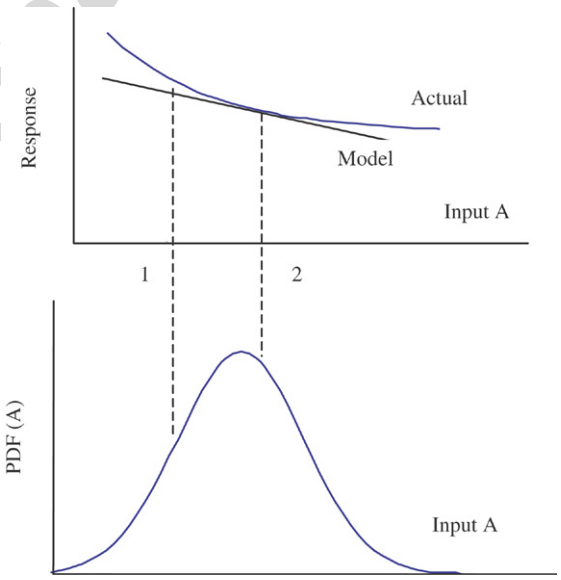

Fig. 1. Collocation points selection in the high probability region (Note: the model is inaccurate at point 1, but corresponds to the region of low probability. The model is accurate at point 2, and corresponds to the region of high probability. Thus point 2 qualifies as a collocation point).

Since there are many possible combinations of the roots, for the higher dimensional and higher order polynomial chaos, the number of available collocation points is always greater than the number of collocation points needed. Therefore, a selection of the appropriate collocation points from the large number of potential candidates is needed. Furthermore, the roots of such a polynomial may not always capture regions of high probability. For example, the origin is not included in the roots of the fourth order polynomial but the origin captures the highest probability for standard normal variables. Therefore, care must be taken to include points from regions of high probability. In addition, it is desirable that the collocation points are close to the origin and be symmetric with respect to the origin [8]. The selected points

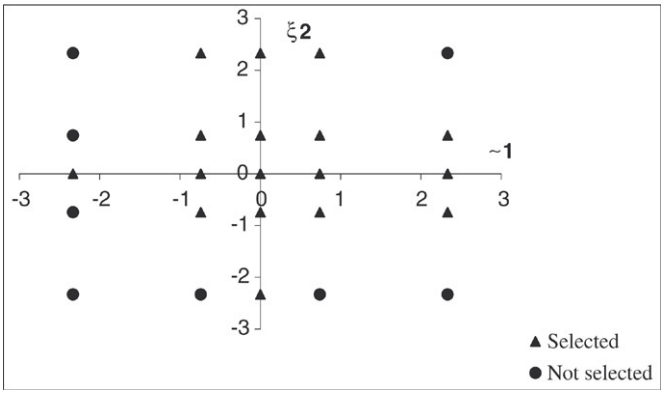

Fig. 2. Selection of collocation points for a third order response surface from combinations of Hermite polynomial roots.

should also give the least regression error for the response surface model. If there are still more points available after incorporating the above guidelines, the remaining collocation points are selected randomly.

According to the above criteria, Table 2 gives the values of the collocation points for the construction of second order and third order response surfaces. Fig. 2 visualizes the collocation points for the third order response surface. In Fig. 2, the sum of "triangle" points and "circle" points is the total number of candidate collocation points which are combinations of the four roots of the fourth order Hermite polynomial and the origin (25 points). The collocation points used for construction of the third order response surface are the 17 "triangle" points. These collocation points are then used to obtain the sample values for the input variables and the response is calculated at these input values. The sampled input and output values are used for regression analysis to estimate the coefficients in the polynomial chaos expansion.

Note that, in the SRSM setting, deterministic finite element analysis is separated from stochastic analysis. The deterministic finite element analysis is performed at each collocation point. Therefore, the size of the system is the same as in the deterministic case. Furthermore, there is no need to reformulate the element stiffness matrix as needed in the analytical version of SSFEM.

3.3. Sample generation

In order to perform the regression analysis to calculate the coefficients in the polynomial chaos expansion, both samples of the input and samples of the output are required. Generation of samples of the random field input is addressed in this subsection. The corresponding samples of the output are then obtained through FEM analysis.

Based on Eq. (8), stochastic simulation of the random field is simplified to finding the Eigenvalues λ_i and Eigenfunctions $f_i(x)$ of the covariance function obtained from the spectral decomposition of the covariance function and generating a set of uncorrelated random variables $\xi_i(\theta)$.

A key step in using the K–L expansion for simulation is to solve for λ_i and $f_i(x)$ via Eq. (4). For the class of covariance functions where Eq. (4) is twice differentiable,

Fig. 3. Cantilever beam.

the differentiation yields a differential equation, which is then solved analytically. Imposing the boundary conditions yields the Eigen-pairs as illustrated by Ghanem [1]. The integral equation can be solved analytically only under special circumstances. In most cases, analytical solution of the integral equation is not tractable and a numerical method is the only recourse. An efficient numerical solution of the second order Fredholm integral equation using wavelets is developed by Phoon et al. [14,15].

The second important step is the selection of uncorrelated standardized K–L random variables $\xi_i(\theta)$. $\xi_i(\theta)$ are selected such that Eq. (8) produces the desired distribution that matches as closely as possible the target marginal distribution function. M is the number of K–L terms that is the control parameter in the accuracy of the K–L expansion. A unified procedure based on the K–L expansion has been developed by Huang [24] to digitally generate sample functions of any non-stationary non-Gaussian process with target covariance function and marginal distribution function. In the case of simulation of a Gaussian field, the algorithm can be greatly simplified since the appropriate choice of $\xi_i(\theta)$ is a vector of zero-mean uncorrelated Gaussian random variables which can be generated by available established subroutines. Simulation of the Gaussian field thus reduces to generating the Gaussian variables $\xi_i(\theta)$, and then multiplying the Eigenfunctions and Eigenvalues as in Eq. (8), derived from Eigen-decomposition of the target covariance model, as in Eq. (4). The value of M is governed by the accuracy of the Eigen-pairs in representing the covariance function. Details involving the simulation of random fields using the K–L expansion can be found in Huang et al. [6], Phoon et al. [14,15], Quek et al. [16] and Huang [24].

4. Numerical study

The implementation of the extended stochastic response surface method is first illustrated with the help of two examples in this section, involving one-dimensional and two-dimensional random fields. Later, the method is compared to the analytical and black-box versions of SSFEM with respect to accuracy and efficiency.

4.1. Beam problem (one-dimensional random field)

A cantilever beam subjected to a concentrated load P (Fig. 3) is considered. It is assumed that the bending rigidity EI of the beam is a Gaussian random process with mean $\mu = \langle EI \rangle = 1$, a finite variance σ^2 and exponential covariance function $C(x_1, x_2)$ of the following type:

$$C(x_1, x_2) = \sigma^2 \mathrm{e}^{-|x_1 - x_2|/b} \tag{27}$$

where σ^2 is the variance and b is the correlation parameter that controls the rate at which the covariance decays. The degree of variability associated with the random process can be related to its coefficient of variation $\delta = \sigma/\mu$. The frequency content of the random process is related to the a/b ratio in which a is the length of the beam. A small a/b ratio implies a highly correlated random field. $a/b = 1$ is chosen in this study. In this example, $\sigma = 0.2$, $b = 1$. The length of the beam is $a = 1$ and it is divided into 10 elements.

The Eigensolutions of the covariance function are obtained by solving the integral equation (Eq. (4)) analytically. The Eigenvalues and Eigenfunctions are given as follows:

$$\lambda_i = \frac{2\sigma^2 c}{\omega_i^2 + c^2} \tag{28}$$

$$\lambda_i^* = \frac{2\sigma^2 c}{\omega_i^{*2} + c^2} \tag{29}$$

$$f_i(x) = \frac{\cos(\omega_i x)}{\sqrt{a + \frac{\sin(2\omega_i a)}{2\omega_i}}} \quad \text{for } i = \text{odd} \tag{30}$$

$$f_i(x) = \frac{\sin(\omega_i^* x)}{\sqrt{a - \frac{\sin(2\omega_i^* a)}{2\omega_i^*}}} \quad \text{for } i = \text{even} \tag{31}$$

where ω_i are found from the following transcendental equations:

$$c - \omega \tan(\omega x) = 0 \tag{32}$$

$$\omega^* + c \tan(\omega^* x) = 0. \tag{33}$$

The random field is discretized into two SRVs, ξ_1 and ξ_2, and the two-term K–L expansion (Eq. (8)) is used to generate sample functions of the input random field. The response quantity which is the tip displacement of the beam is represented by a polynomial chaos expansion. A second order polynomial chaos expansion with two SRVs is constructed with the basis defined in Eq. (13). For regression-based SRSM, 9 sample points are selected to estimate the 6 unknown coefficients in the second order polynomial chaos expansion [8]. These sample points, as discussed earlier, are the roots of a Hermite polynomial of the third order. These values are then substituted into Eq. (8) to calculate sample functions of the random field which is the bending rigidity of the beam. For each sample function of the bending rigidity, the corresponding response (tip displacement) is computed. The set of values of y and ξ_1, ξ_2 are used in regression to obtain the coefficients of the polynomial chaos expansion. A third order response surface is constructed with 17 sample points for SRVs. The collocation points for the second order and third order response surfaces are shown in Table 2.

To evaluate the validity of the results obtained from the proposed method and to test the convergence property, Monte Carlo simulation is performed for the same problem. Realizations of the bending rigidity of the beam are numerically simulated using the K–L expansion method. For each of the realizations, the deterministic problem is solved and

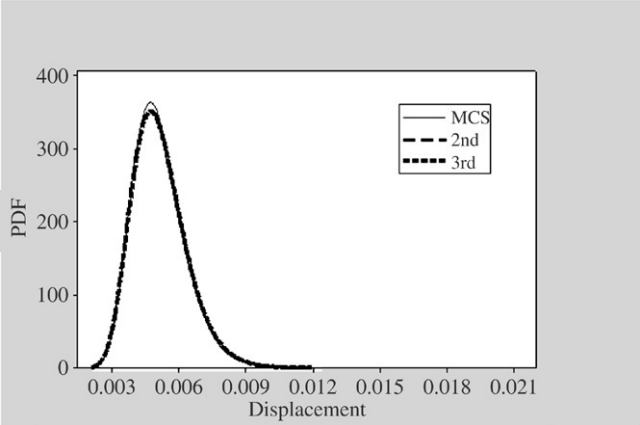

Fig. 4. Probability density function for beam tip displacement.

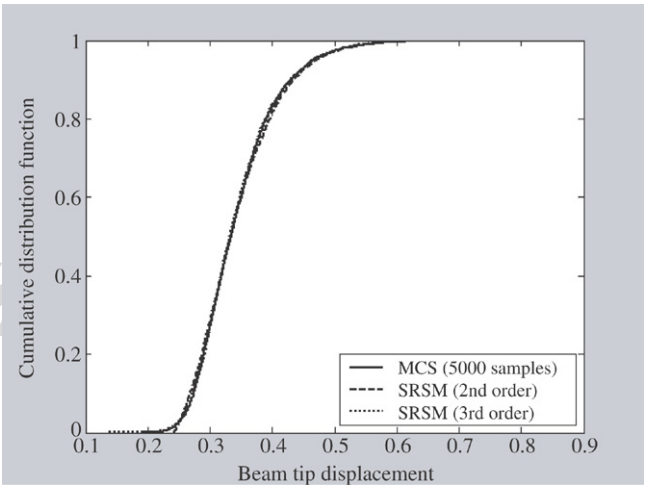

Fig. 5. Cumulative distribution function for beam tip displacement.

the statistics of the response are obtained. Fig. 4 shows the probability density functions obtained from Monte Carlo simulation and SRSM with two K–L variables. SRSM results converge to the Monte Carlo simulation result. A good agreement is observed between the third order stochastic response surface result and 5000 Monte Carlo simulation results The cumulative distribution function is shown in Fig. 5.

It should be noted that K–L expansion with two terms is not enough for an accurate representation of the input random field (even for a highly correlated field, e.g. $a/b = 1$). It has been shown that for a random field with $a/b = 1$, a two-term representation may give 30%–50% error in the variance of the discretized field [9]. According to the detailed convergence study by Huang et al. [6], 10 terms or more would be necessary for an accurate representation, which will result in a large number of FE runs. SSFEM has the same problem in the sense that the computational effort increases dramatically with the number of terms in the K–L expansion. As the same K–L expansion is used for Monte Carlo simulation and SRSM, the inaccuracy in input random field does not show in the results. However, the purpose of this paper is to show that SRSM can work as well as Monte Carlo simulation with much less FE

runs. The inaccuracy in input random field for both methods is acknowledged.

4.2. Plate problem

A square plate subjected to deterministic uniformly distributed load w_1 and w_2 is considered. In this example, making use of symmetry, only a quarter of the plate is analyzed, as shown in Fig. 6. In this problem, the elasticity modulus E of the plate is assumed to be a two-dimensional homogeneous Gaussian random field, with mean $\overline{E} = 10^4$, and exponential covariance function $C(x_1, y_1; x_2, y_2)$ reflecting the correlation of the random field at any two points (x_1, y_1) and (x_2, y_2) on the plate. The covariance function is of the following type:

$$C(x_1, x_2) = \sigma_E^2 \mathrm{e}^{-|x_1-x_2|/b_x} \mathrm{e}^{-|y_1-y_2|/b_y} \tag{34}$$

where b_x and b_y are the correlation distances in x and y directions respectively. σ_E is the standard deviation of E ($=0.2 \times 10^4$). In this example, making use of symmetry, only a quarter of the plate is analyzed, as shown in Fig. 6. In Fig. 10, $l_x = l_y = 12$ and $b_x = b_y = 12$. The thickness of the plate is 1 and Poisson's ratio is 0.2. The loading is deterministic and $w_1 = w_2 = 12$. The plate is divided into 133 elements and the Eigensolutions of the covariance function are obtained by solving the integral equation analytically:

$$\lambda_n f_n(x_1, y_1) = \int_{-l_x/2}^{l_x/2} \int_{-l_y/2}^{l_y/2} C(x_1, y_1; x_2, y_2) f_n(x_2, y_2) \mathrm{d}x_1 \mathrm{d}y_1. \tag{35}$$

Substituting Eq. (34) for the covariance function and assuming the Eigensolution is separable in x and y directions, i.e.,

$$f_n(x_1, y_1) = f_i^{(x)}(x_1) f_j^{(y)}(y_1) \tag{36}$$

and

$$\lambda_n = \lambda_i^{(x)} \lambda_j^{(y)}. \tag{37}$$

The solution of Eq. (35) reduces to the product of the solutions of two equations of the form

$$\lambda_i^{(x)} f_i^{(x)}(x_1) = \int_{-l_x/2}^{l_x/2} \mathrm{e}^{-|x_1-x_2|/b_x} f_i^{(x)}(x_2) \mathrm{d}x_2. \tag{38}$$

The solution of this equation, which is the Eigensolution of an exponential covariance kernel for a one-dimensional random field, is given in Section 4.1. In the final expression for the Eigenfunctions, it should be noted that two functions of the form given by Eq. (38) correspond to each Eigenvalue. The second one is obtained from the first one by permuting the subscripts. The final Eigenfunctions are given by

$$f_n(x, y) = f_i^{(x)}(x) f_j^{(y)}(y). \tag{39}$$

After obtaining the Eigensolutions, the random field is discretized into two SRVs, ξ_1 and ξ_2 and this two-term K–L expansion is used to generate sample functions of the input random field. The response quantity, which is the vertical displacement at a particular node (Point A), can be represented by a polynomial chaos expansion. Using the same sample points in Table 2, nine sample functions for E are generated for constructing a second order response surface.

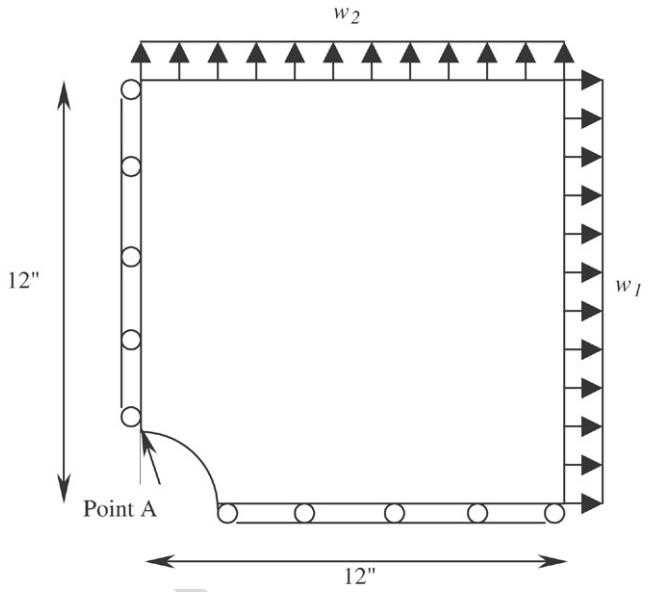

Fig. 6. Simplified computation model of square plate with a circular hole.

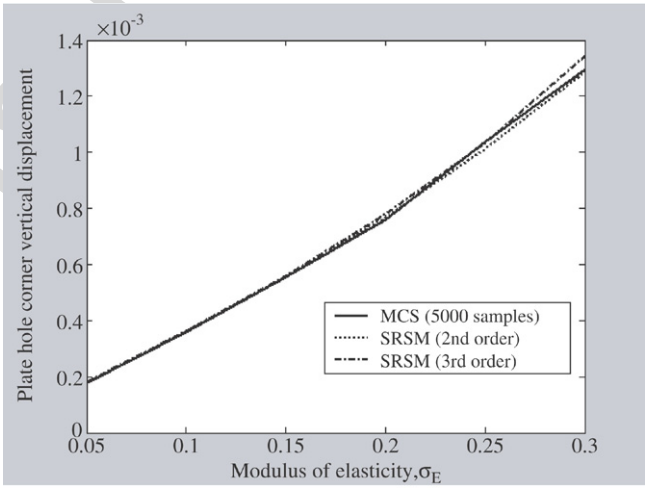

Fig. 7. Standard deviation of plate hole corner vertical displacement vs. standard deviation of modulus of elasticity.

Fig. 7 shows the standard deviation of the response quantity versus that of the modulus of elasticity for different orders of the stochastic response surface from SRSM and Monte Carlo simulation. A good agreement is shown for relative small values of the coefficient of the variation δ. With fixed $\delta = 0.3$, the second order response surface from SRSM is

$$\begin{aligned} Y = {} & 0.004891 - 0.00019\xi_1 - 5.9 \times 10^{-7}\xi_2 \\ & + 7.32 \times 10^{-6}(\xi_1^2 - 1) - 8.9 \times 10^{-9}(\xi_2^2 - 1) \\ & + 4.67 \times 10^{-8}\xi_1\xi_2. \end{aligned} \tag{40}$$

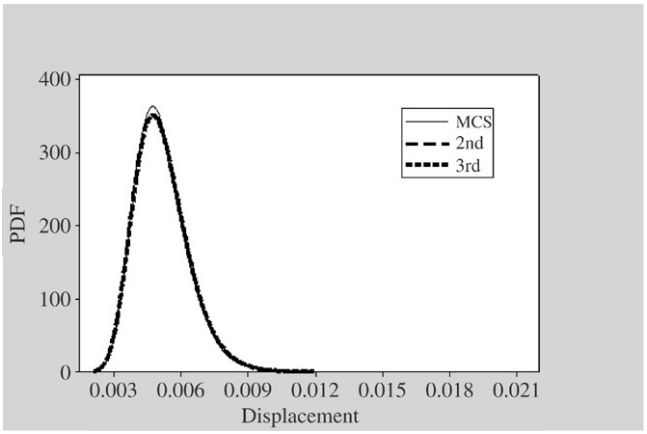

Fig. 8. Probability density function for the vertical displacement at point A of the plate.

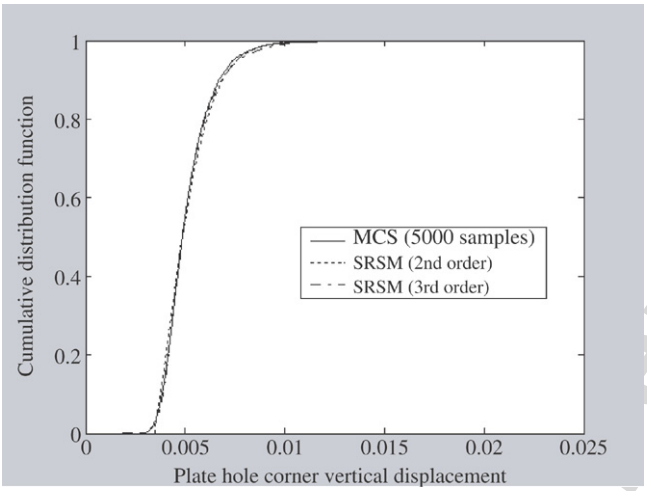

Fig. 9. Cumulative distribution function of the plate hole corner vertical displacement.

The third order response surface constructed with 17 sample points is

$$\begin{aligned} Y = {} & 0.004891 - 0.00019\xi_1 - 5.6 \times 10^{-7}\xi_2 \\ & + 7.32 \times 10^{-6}(\xi_1^2 - 1) + 1.47 \times 10^{-7}\xi_1\xi_2 \\ & - 6.9 \times 10^{-11}(\xi_2^2 - 1) - 2.9 \times 10^{-7}(\xi_1^3 - 3\xi_1) \\ & + 4.6 \times 10^{-8}(\xi_1^2\xi_2 - \xi_2) - 6 \times 10^{-8}(\xi_2^2\xi_1 - \xi_1) \\ & + 3.03 \times 10^{-9}(\xi_2^3 - 3\xi_2). \end{aligned} \tag{41}$$

Figs. 8 and 9 show the probability distributions obtained from Monte Carlo simulation and SRSM with two K–L variables. A good agreement is observed between the results from stochastic response surface and Monte Carlo simulation (5000 samples).

4.3. Numerical comparison of SRSM and SSFEM

To compare the performance of the extended SRSM and two versions of the spectral stochastic finite element method, the cantilever beam in Section 4.1 is used, with a deterministic uniformly distributed load q.

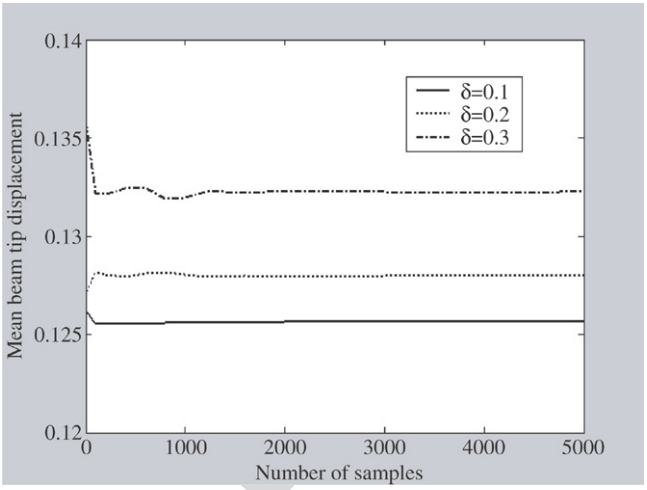

Fig. 10. Convergence of mean beam tip displacement (Monte Carlo simulation).

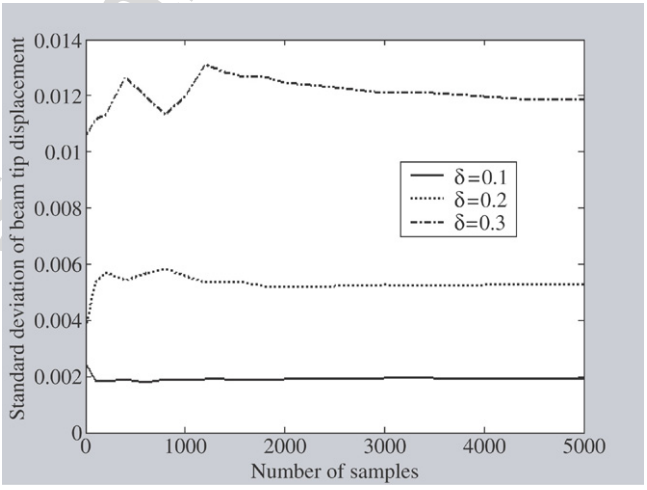

Fig. 11. Convergence of the standard deviation of beam tip displacement (Monte Carlo simulation).

Various values of δ are considered in this example. To evaluate the validity of the results obtained from the proposed method, Monte Carlo simulation is performed for the same problem. Realizations of the bending rigidity of the beam are numerically simulated using the K–L expansion method. For each of the realizations, the deterministic problem is solved and the statistics of the response are obtained. In Figs. 10 and 11, expected values and standard deviation of the displacement at the tip obtained by Monte Carlo simulation are presented. It is observed that for $\delta < 0.2$, 500 simulations are sufficient to obtain the convergence. When $\delta \geq 0.2$, it is necessary to increase the number of simulations.

Fig. 12 plots the standard deviation of tip displacement σ_u versus the standard deviation of bending rigidity of the beam σ_{EI} for different orders of the stochastic response surface, and Monte Carlo simulation. A good agreement is shown for relatively small values of the coefficient of variation δ. Fixing $\delta = 0.3$, Fig. 13 shows the cumulative distribution functions obtained from Monte Carlo simulation and SRSM with two

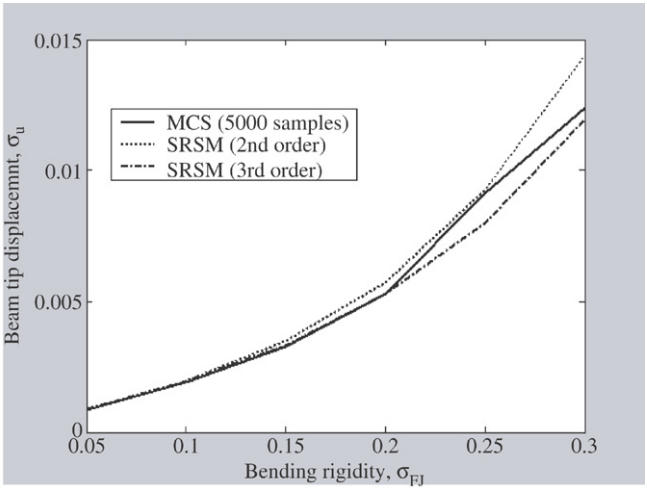

Fig. 12. Standard deviation of beam tip displacement versus standard deviation of bending rigidity.

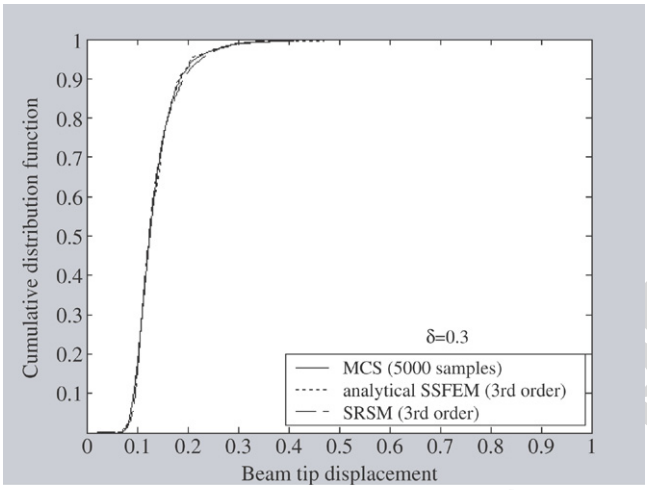

Fig. 13. Comparison of cumulative distribution functions for SRSM and analytical SSFEM.

K–L variables. A good agreement is observed between the third order stochastic response surface and Monte Carlo simulation (5000 samples). The analytical SSFEM results [1] also show good agreement. Thus it can be concluded that SRSM can achieve satisfactory results just as in analytical SSFEM, without the significant programming effort to change the existing finite element code. The results from third order SRSM (17 samples) and black box SSFEM (100 samples) are shown in Fig. 14. It is seen that SRSM achieves better result using less samples than the Latin Hypercube sampling-based black-box SSFEM for this numerical example.

5. Conclusion

This paper presented an extended stochastic response surface method for problems in which physical properties exhibit spatial random variation, by using collocation points as samples for constructing the output response surface. The method appears to be efficient, requiring only several

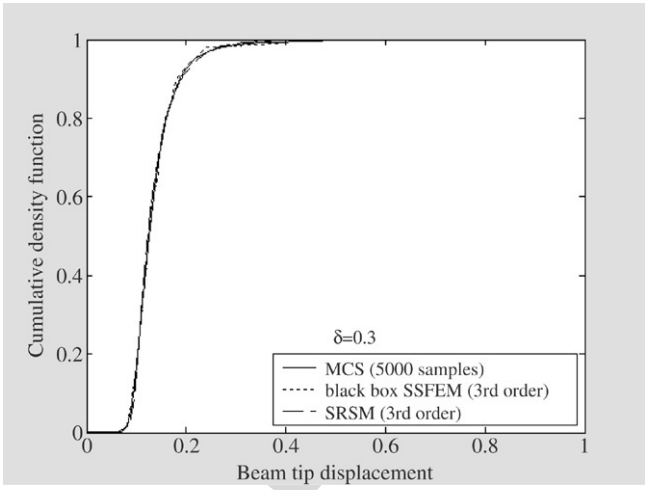

Fig. 14. Comparison of cumulative distribution functions for SRSM and black-box SSFEM.

runs or tens of runs to accurately compute the solution statistics. In comparison, Monte Carlo simulation may require thousands of realizations or more for converged statistics. Thus the proposed method substantially reduces the computational effort while maintaining the desired accuracy. However, for random field input that is weakly correlated, SRSM requires a K–L expansion with many terms, which may increase the dimensionality and thus the computational effort of the method. However, it should be remembered that out of all random field simulation techniques currently available in the literature, K–L expansion requires the least number of standard random variables and hence the method is still effective. Also, the curse of dimensionality is not limited to the proposed collocation-based SSFEM; it is a problem in other currently available methods as well.

Also, the proposed method is independent of the structural analysis and treats the finite element model as a black-box. If higher loads introduce nonlinearity in the model response, then the appropriate nonlinear analysis should be used, and the underlying response surface would automatically be different. Thus the proposed method is applicable to the analysis of linear as well as nonlinear structures, provided the right 'black-box' is used.

Comparison of numerical results between the extended SRSM and the two versions of SSFEM (analytical and black-box) reveals that each method has its own advantages and disadvantages. The following observations are made in comparing the two SSFEM approaches and the extended SRSM approach:

(1) *Programming effort*: Both SRSM and the black-box SSFEM treat the finite element code as a black-box, as in the case of a commercial code, whereas analytical SSFEM requires significant programming effort to change the existing finite element code. This advantage of SRSM becomes increasingly valuable as the physical problem increases in complexity and size.
(2) *Computational effort*: Analytical SSFEM uses only one run to obtain the stochastic response surface while SRSM and

black-box SSFEM need more runs. However, the size of the system in analytical SSFEM is larger than in the other two methods. Depending on the problem, either approach may be computationally more efficient than the other. Although both the black-box SSFEM and SRSM use the FEM code as a black-box, SRSM (based on collocation points) may require much fewer samples to calculate the coefficients in the response surface than the black-box SSFEM which uses random sampling such as Latin Hypercube sampling.

(3) *Handling spatial variability*: Both SSFEM and SRSM can accurately handle random fields with large coefficients of variation unlike other methods such as perturbation and Neumann expansion methods. However, both SSFEM and SRSM are computationally efficient only when random fields are strongly correlated because both use the K–L expansion which requires only a few terms to represent strongly correlated random fields.

Acknowledgments

The research reported in this paper was supported by funds from Sandia National Laboratories, Albuquerque, NM (Contract No. BG-7732), under the NSF-Sandia Life Cycle Engineering Program (Project Monitor: Dr. Steve Wojtkiewicz). The support is gratefully acknowledged. Sandia is a multi-program laboratory operated by Sandia Corporation, a Lockheed Martin Company, for the U.S. Department of Energy under Contract DE-AC04-94AL85000.

References

[1] Ghanem R, Spanos PD. Stochastic finite elements: A spectral approach. Springer-Verlag; 1991.

[2] Ghanem R, Kruger R. Numerical solution of spectral stochastic finite element systems. Computer Methods in Applied Mechanics and Engineering 1996;129:289–303.

[3] Ghanem R, Spanos PD. Spectral techniques for stochastic finite elements. Archives of Computational Methods in Engineering 1997;4(1):63–100.

[4] Ghanem R. Ingredients for a general purpose of stochastic finite element formulation. Computer Methods in Applied Mechanics and Engineering 1999;168(1–4):19–34.

[5] Ghiocel D, Ghanem R. Stochastic finite element analysis of seismic soil–structure interaction. Journal of Engineering Mechanics ASCE 2002; 128(1):66–77.

[6] Huang SP, Quek ST, Phoon KK. Convergence study of the truncated Karhunen–Loeve expansion for simulation of stochastic processes. International Journal for Numerical Methods in Engineering 2001;52: 1029–43.

[7] Iman RL, Conover WJ. A distribution free approach to introducing rank correlation among input variables. Communication on Statistics—Simulation and Computation 1982;11(3):311–34.

[8] Isukapalli SS, Roy A, Georgopoulos PG. Stochastic response surface methods (SRSMs) for uncertainty propagation: Application to environmental and biological systems. Risk analysis 1998;18(3):351–63.

[9] Li CC, Der-Kiureghian A. Optimal discretization of random process. Journal of Engineering Mechanics ASCE 1993;119(6):1136–54.

[10] Li R, Ghanem R. Adaptive polynomial chaos simulation applied to statistics of extremes in nonlinear random vibration. Probabilistic Engineering Mechanics 1998;13(2):125–36.

[11] Liu WK, Belytschko T, Mani A. Random field finite elements. International Journal for Numerical methods in Engineering 1986;23: 1831–45.

[12] McKay MD, Beckman RJ, Conover WJ. A comparison of three methods for selecting values of input variables in analysis of output from a computer code. Technometrics 1979;2:239–45.

[13] Pellissetti M, Ghanem R. Iterative solution of systems of linear equations arising in the context of the stochastic FEM. Journal of Advances in Engineering Software 2000;31:607–16.

[14] Phoon KK, Huang SP, Quek ST. Simulation of non-Gaussian processes using Karhunen–Loeve expansion. Computers & Structures 2002;80: 1049–60.

[15] Phoon KK, Huang SP, Quek ST. Implementation of Karhunen–Loeve expansion for simulation using a wavelet-Galerkin scheme. Probabilistic Engineering Mechanics 2002;17:293–303.

[16] Quek ST, Huang SP, Phoon KK. A unified procedure for simulating second-order stochastic processes. In: First M.I.T. conference on computational fluid and solid mechanics. Massachusetts Institute of Technology; 2001.

[17] Tatang MA, Pan W, Prinn RG, McRae GJ. An efficient method for parametric uncertainty analysis of numerical geophysical models. Journal of Geophysical Research 1997;102(D18):21925–32.

[18] Yamazaki F, Shinozuka M. Neumann expansion for stochastic finite element analysis. Journal of Engineering Mechanics ASCE 1988;114(8): 1335–54.

[19] Van Trees HL. Detection, estimation and modulation theory, Part 1. New York: John Wiley & Sons; 1968.

[20] Vanmarcke E, Grigoriu M. Stochastic finite element analysis of simple beams. Journal of Engineering Mechanics ASCE 1983;109:1203–14.

[21] Villadsen J, Michelsen ML. Solution of differential equation models by polynomial approximation. Englewood Cliffs (NJ): Prentice-Hall; 1978.

[22] Xiu D, Karniadakis GE. Modeling uncertainty in flow simulations via generalized polynomial chaos. Journal of Computational Physics 2001.

[23] Schoutens W. Stochastic processes and orthogonal polynomials. New York: Springer; 2000.

[24] Huang S. Simulation of random processes using Karhunen–Loeve expansion. Ph.D. thesis. National University of Singapore, Singapore; 2001.